九州大学学術情報リポジトリ
Kyushu University Institutional Repository

Preliminary Modeling of Coupled Motion Response for Floating Crane and Suspended Module by Using Boundary Element Approach and Empirical Model

Firdaus, Nurman
Research Center for Hydrodynamic Technology, National Research and Innovation Agency, Indonesia

Ali, Baharuddin
Hydrodynamics Laboratory, National Research and Innovation Agency, Indonesia

Hidayat, Affan
Hydrodynamics Laboratory, National Research and Innovation Agency, Indonesia

Zainul Khaqiqi Nantabah
Hydrodynamics Laboratory, National Research and Innovation Agency, Indonesia

他

https://doi.org/10.5109/7151718

出版情報：Evergreen. 10 (3), pp.1695-1707, 2023-09. Interdisciplinary Graduate School of Engineering Sciences, Kyushu University, Japan
バージョン：
権利関係：Creative Commons Attribution-NonCommercial 4.0 International

KYUSHU UNIVERSITY

Preliminary Modeling of Coupled Motion Response for Floating Crane and Suspended Module by Using Boundary Element Approach and Empirical Model

Nurman Firdaus[1,*], Baharuddin Ali[2], Affan Hidayat[2], Zainul Khaqiqi Nantabah[2], E.B. Djatmiko[3], Rudi Walujo P.[3]

[1]Research Center for Hydrodynamic Technology, National Research and Innovation Agency, Indonesia

[2]Hydrodynamics Laboratory, National Research and Innovation Agency, Indonesia

[3]Department of Ocean Engineering, Sepuluh Nopember Institute of Technology Surabaya, Indonesia

*Author to whom correspondence should be addressed:
E-mail: nurm006@brin.go.id

(Received February 15, 2023; Revised June 26, 2023; accepted July 9, 2023).

Abstract: External forces and environments can destabilize the floating crane's performance and inflict a high risk of failure in operation. Considering this, the effect of the suspended module during the lifting operation in sea waves is investigated to evaluate the dynamic response of the floating crane. In this article, the combination of potential flow theory in the Boundary Element Method (BEM) and an empirical model is proposed for the prediction of coupled motion on the floating crane and suspended module. Calculations of multibody systems are solved using the coupled motion formula based on the frequency domain method. An analysis of the lifting operation under beam waves is examined with two variations in the weight of the suspended module. The motion characteristics are depicted with the response amplitude operator (RAO) on the nine rigid body degrees of freedom. The resonances of peak frequency occurred in the floating crane's responses due to the lifting load system. The peak frequency of the roll response on the floating crane shifted to a higher frequency due to the impact of the pendulum motion. The difference in peak response of roll motion between variations of suspended load is about 25.8 %. The acceleration response of the suspended module in the z-direction for the large module presented a lower peak frequency than the smaller module.

Keywords: modeling; coupled motion; floating crane; waves

1. Introduction

The country's potential income from the maritime business sector will develop rapidly if many activities use the infrastructure of a floating crane. The cranes are utilized to support the loading and unloading of transportation from ships to ships or barge to ships in offshore or port areas[1)]. This infrastructure supports the economic acceleration of the marine industry cluster. The floating crane is designed to be placed in the middle of the sea for flexible and efficient operations[2)]. So, the demand for lifting operations using floating cranes was increasing significantly.

The challenges encountered during the handling of payloads by crane vessels are instability due to the external environment. Lifting a load in the water has risks and operational failures caused by the unstable motion response of the floating crane. The stability of floating cranes has a significant effect on the safety of handling global operations at sea[3)]. During a lifting operation, the dynamic response of a floating crane is very sensitive due to small wave conditions. Moreover, the excitation force of the floating crane is getting bigger due to the coupling motion with the lifted object. According to Firdaus et al.[4)], using a floating crane on a sea wave has limited safety criteria for the lifting process.

Several researchers and practitioners have investigated the effect of pendulum motion on floating crane motion for several decades. Mukerji[5)] has demonstrated the effect of a hanging load on the derrick vessel based on a linearized formulation. The simulation result showed that the lifted objects, which account for about 5% of the ship's weight, have a significant effect on the ship's motion. Baar et al.[6)] have calculated the dynamic response between the crane vessel and transport barge during offshore lifting due to hydrodynamic interaction effects. The results of the numerical model using the coupling equation stated that the hoisting wire and slings cause the effect of mechanical coupling on the vessel response. Meanwhile, Li et al.[7)] conducted a numerical simulation

of the offshore lifting for a monopile on the wind turbine. Their research indicated that the monopile motion affects the resonance of the crane vessel's response. An experimental study of floating crane barges with and without a lifted load was investigated by Firdaus et al.[8]. The results of the model test show that the movement of the lifted load influences the roll response and the shift of the natural period.

The numerical models are constantly developing in lifting operations due to the non-negligible interaction between the crane ship's motion response and the suspended load. Witz[9] investigated the nonlinear response of the offshore lift using a time-domain method. The length of the suspended load rope affects the dominant parametric excitation. Other authors, Idres et al.[10], examined the dynamic models of crane vessels coupled with lifted cargo. By using their formulation method, the ship's motion has a strong impact on the cargo oscillations. Coric et al.[11] studied the multibody motion interaction between a floating crane and a swinging pendulum using the linear model. In the results of transfer functions, there is a frequency resonance in the rolling motion due to the oscillation of the suspended module. Chen et al.[12] explained that the length of cable on the suspended human-occupied vehicle (HOV) has a clear influence on the mother ship's response in the launching process, which is calculated using an experimental method.

The effect of the lifted caissons on the dynamic response of the floating crane was investigated using a numerical model and field measurements by Oh et al.[13]. Numerical models are commonly developed for the dynamic response between the floating crane and the suspended load in sea waves. Previous authors with similar topics have discussed cases of coupled motion during lifting operations, which are listed in Table 1.

Table 1. Summarized References of Milestone Studies.

Authors	Title	Method	Parameters
P.K. Mukerji[5]	Hydrodynamic Response of Derrick Vessels in Waves During Heavy Lift Operation	Numerical model	• The multibody system has 8 degrees of freedom. • Unified analysis
J.J.M. Baar, J.G.L Pijfers[6]	Hydromechanically Coupled Motions of a Crane Vessel and a Transport Barge	Numerical calculation (in-house code)	• With and without hydrodynamic interaction, slack and taut slings in two vessels • Diffraction analysis • Wave directions
J.A. Witz[9]	Parametric Excitation of Crane Loads in Moderate Sea States	Numerical program (in-house code)	• Time domain integration • Five degrees of freedom coupling between the vessel and crane load • Pierson-Moskowitz spectrum in a head sea
M.M. Idres, K.S. Youssef, D.T. Mook, A.H. Nayfeh[10]	A Nonlinear 8-DOF Coupled Crane-Ship Dynamical Model	Computer simulation (in-house code)	• Six degrees of freedom in ship motion and two degrees of freedom in crane cargo • Regular and irregular waves
Veceslav Coric, Ivam Catipovic, Vedran Slapnicar[11]	Floating Crane Response in Sea Waves	Numerical model and model test in a Towing Tank	• Six degrees of freedom of floating crane and three degrees of freedom of swinging load • Scaling parameter • Significant response and transfer function
Sho Oh, Tomoaki Utsunomiya, Kota Saiki[13]	On-Site Measurement and Numerical Modelling of a Lifting Operation for Caissons Using Floating Crane	Numerical model and On-Site Observation	• Frequency domain analysis • Full-scale ratio • Roll and pitch motion • Cargo acceleration in y and x directions

Yunsai Chen, Liang Ma, Wenyang Duan, Peng Liu[12)]	Experimental Study on Coupled Motions of Mother Ship Lunching and Recovering of Human-Occupied Vehicle in Regular Waves	Model test in wave tank	• Scaling Ratio • Regular waves • Head and beam seas • Cable length variations
Nurman Firdaus, Eko Budi D., Rudi Walujo P., Muryadin[8)]	Experimental Study on Coupled Motion of Floating Crane Barge and Lifted Module in Irregular Waves	Experimental in Ocean Basin	• Scaling Model • Irregular waves variations • Wave frequency

Corresponding to previous research in this article, this study aims to propose an accurate estimation of the dynamic response to interaction effects between the floating crane and the suspended module with simple preliminary modeling. The wave load can raise a large resonance and then cause the floating crane to capsize during lifting operations. Meanwhile, the floating crane experiences an overexcitation response by considering the external load from the oscillation of the suspended module. This study focuses on the effects of suspended modules, including the 9-DOF model coupled lifting system and floating crane barge, on safe operation in sea waves. The present article analyzes the method for approximation support systems during the lifting process in the maritime industry based on hydrodynamic coefficients from potential flow theory and the empirical model.

2. Methodology

The calculation of a multibody system for lifting operations conducted by standby conditions in waves is important for identifying the interaction between two rigid bodies. The numerical simulation using an in-house program is developed to predict dynamic responses efficiently and quickly. The equation of coupled motion for two bodies connected by a hoisting rope consists of a 6-DOF floating crane and a 3-DOF lifting system. The hydrodynamic coefficients of floating barges are obtained from the calculation using the 1st-order potential theory of the boundary element method (BEM). The response model of 6 DOF is calibrated with the program result code of BEM. In this study, the response amplitude operator of the lifting system is investigated only under regular beam sea and two variations of lifted modules. The dynamic responses are presented and analyzed using frequency-domain analysis.

2.1 Mathematical Modeling

The proposed coupling motion equations for lifting operations using floating cranes are given in this part. The prediction in this study considers the linear differential equation of motion because it is derived by assuming a small floating crane and suspended load excursion. The equation of coupled motion of system analysis in nine degrees of freedom can be written as in Equation 1.

$$(M + A(\omega))\ddot{x} + (B + B_v)\dot{x} + (C_h + C_m + C_c)x = F_w \quad (1)$$

Where (ω) denotes the wave frequency; $\ddot{x}$, $\dot{x}$, and x are nine component column vectors of acceleration, velocity, and displacement; x consists of surge, sway, heave, roll, pitch, and yaw motions of the floating crane, together with x, y, and z direction motions of the suspended module, respectively; $(M + A)$ are composed of the total mass and inertia mass plus the added mass and inertia of the floating crane together with the suspended module mass, the added mass of module is zero because the position of suspended load is assumed to be above the water surface; $(B + B_V)$ are the hydrodynamic plus the viscous damping of the floating crane along, with the structural damping of the suspended system; C_h is the hydrostatic stiffness matrix of the floating crane, C_m is a linearized mooring restoring force matrix and C_c is the linear coupled stiffness matrix due to the interaction of the suspended system body; F_W is the force and moment of incident wave excitation, including the first order wave excitation. In this investigation, only the environmental wave excitation force on the floating crane hull is included in the simulation model; the excitation forces from other environmental conditions are neglected.

The generalized mass and inertia matrices of two rigid bodies in a multibody system can be written as follows:

$$\begin{bmatrix} (M_S + A) & & O & \\ & M_L & 0 & 0 \\ O & 0 & M_L & 0 \\ & 0 & 0 & M_L \end{bmatrix} \quad (2)$$

Where M_S represents the mass and inertia matrix (6 x 6) of the rigid body of the floating crane in the six rigid body degrees of freedom of surge, sway, heave, roll, pitch, and yaw. The masses of the fixed crane boom and suspended module are included in the total mass of the floating crane. M_L is the mass of the suspended load during lifting operations in the three degrees of freedom of the rigid body. Furthermore, the ballast condition of the floating crane during the lifting process is assumed to be on an even keel in this study.

The frequency-dependent linearized hydrodynamic added mass and damping coefficient matrices for the total lifting system using a floating crane can be written as

follows:

$$\begin{bmatrix} A & 0 & 0 & 0 \\ 0 & 0 & 0 & 0 \\ 0 & 0 & 0 & 0 \\ 0 & 0 & 0 & 0 \end{bmatrix} \quad (3)$$

$$\begin{bmatrix} (B+B_v) & 0 & 0 & 0 \\ 0 & b_x & 0 & 0 \\ 0 & 0 & b_y & 0 \\ 0 & 0 & 0 & b_z \end{bmatrix} \quad (4)$$

Where A is the hydrodynamic added mass coefficient matrix (6 x 6) for a rigid body of a floating crane in six degrees of freedom. $(B + B_V)$ are the hydrodynamic linear and viscous damping coefficient matrix (6 x 6) for a rigid body of a floating crane in the six degrees of freedom.

According to Siow et al.[14], a simple equation for viscous damping around the submerged hull of a floating crane can be approximated by the following equation:

$$B_V = v\left(\left(M_S + A\right)\omega_n\right)C_h \quad (5)$$

Where v denotes the damping ratio. The value of ratio damping for barges is about 1 - 5%[15]. ω_n is the natural frequency matrix of each rigid body. The term of hanging system damping for b_x, b_y, and b_z are taken here as 1%, 1%, and 5 % of the critical damping in the x, y, and z direction motions, respectively. The hydrodynamic coefficients of added mass and linear damping of the floating crane body were obtained by ANSYS AQWA, which utilized the 3-D panel method, ANSYS[16]. This includes the calculation of the excitation forces and moments on the floating hull. The added mass coefficient, damping coefficient, and excitation force are based on the wave frequency, respectively.

The hydrostatic and mooring restoring stiffness matrix on the system can be written as follows:

$$\begin{bmatrix} (C_h + C_m) & 0 & 0 & 0 \\ 0 & 0 & 0 & 0 \\ 0 & 0 & 0 & 0 \\ 0 & 0 & 0 & 0 \end{bmatrix} \quad (6)$$

Where $C_h + C_m$ is the hydrostatic stiffness and linearized mooring restoring forces (6 x 6) for the rigid body of the floating crane in six rigid bodies with all remaining terms being zero.

The coupled motion between the floating crane and the suspended module is affected by the oscillatory response of the sling. This interaction is created by the elastic hoisting rope at the end of the crane tip and the link in the lifted module. Therefore, the linear coupling stiffness matrix is given by Det Norske Veritas[17]:

$$\begin{bmatrix} k_s & 0 & 0 & 0 & k_s z_p & -k_s y_p & -k_s & 0 & 0 \\ & k_s & 0 & -k_s z_p & 0 & k_s x_p & 0 & -k_s & 0 \\ & & k_e & k_e y_p & -k_e x_p & 0 & 0 & 0 & -k_e \\ & & & c_{c44} & -k_e x_p y_p & -k_e z_p x_p & 0 & k_s z_p & -k_e y_p \\ & & & & c_{c55} & -k_s z_p y_p & -k_s z_p & 0 & k_e z_p \\ & & & & & c_{c66} & k_s y_p & -k_s z_p & 0 \\ & & & & & & k_s & 0 & 0 \\ & & & & & & & k_s & 0 \\ & & & & & & & & k_e \end{bmatrix} \quad (7)$$

Where (x_p, y_p, z_p) are the coordinates of the suspended module's position relative to the center of gravity of the floating crane barge. k_e is the vertical restoring force of the crane boom and the suspension wire load. k_s is the transverse restoring force of the swinging module on the suspension line.

The two restoring forces due to gravity and the axial stiffness of the hoisting rope, respectively, can be written as in Equations 8-10:

$$k_s = \frac{M_L g}{l_s} \quad (8)$$

$$k_e = \frac{A_0 E}{l_e} \quad (9)$$

$$l_e = \frac{M_L \cdot g \cdot l_s}{A_0 E} \quad (10)$$

Where g denotes the gravitational acceleration; l_s is the outstretched length of the hoisting rope, which means the distance between the crane tip and the center of gravity of the suspended module; l_e is the effective length of the elastic hoisting rope; A is the area of the hoisting rope; and E is Young's modulus of elasticity of the hoisting rope.

Meanwhile, the area of rope can be simply defined as follows:

$$A_0 = \frac{\pi . D^2}{4} C_f \tag{11}$$

Where D is the diameter of the hoisting rope, Young's modulus of elasticity is assumed to be taken as $E = 196.10^9$ Pa, and C_f is the filling coefficient of the rope, which is assumed to be taken as 0.58.

For the coupling stiffness equation on the floating crane motion in roll/roll, pitch/pitch, and yaw/yaw, the equation can be described again as follows:

$$c_{c44} = k_s z_p^2 + k_e y_p^2 \tag{12}$$

$$c_{c55} = k_s z_p^2 + k_e x_p^2 \tag{13}$$

$$c_{c66} = k_s \left(x_p^2 + y_p^2 \right) \tag{14}$$

2.2 Model Description

In this article, the system modeling is calculated numerically using a computer program. The research on simulation models conducted by most researchers and academicians uses many empirical models to verify theories and solve complex calculations[18,19]. The floating crane design used in the simulation model is a barge-shaped structure that can be called a floating crane barge. The simple floating crane barge system is shown in Fig. 1. To develop numerical calculations and the distribution of mass properties in this study, the lifted load is simplified as a rectangular box. The floating crane barge adjusts the stable structure during the lifting process, while the suspended module response influences the motion of the floating crane barge. The model system includes two rigid bodies coupled through the hoisting rope. The structure of the crane boom is rigidly fixed to a floating barge. The mooring line is attached to each corner of the hull of the floating barge.

The principal dimensions and mass properties of the floating crane and suspended module are listed in Table 1. The barge hull has a length of 84 m, a breadth of 21 m, and a draft of 2.5 m. The weight of the floating system is about 3469 metric tons. In this study, the weight of the suspended module was between 3.3% and 6.7% of the floating crane barge. The outstretched length of the hoisting rope during the simulation is about 34 m. The suspended modules are placed above the surface water level at a distance of 10.3 m in height.

The global coordinate system (Earth-frame) applies a right-hand coordinate system with the following orientation: the X direction is towards the bow, the Y direction is towards the port side, and the Z direction points upward. The origin of the barge is used as a reference for calculating hydrodynamic coefficients and hydrodynamic and hydrostatic forces. The origin is located on the centerline, mean waterline, and amidship section. The modes of module motion along the x, y, and z axes are denoted by the orientation of the floating barge, respectively. The coordinate system of the direction of multibody motion at the nine DOF in this simulation can be seen in Fig. 2. The crane tip is perpendicular to the coordinate system of the suspended module.

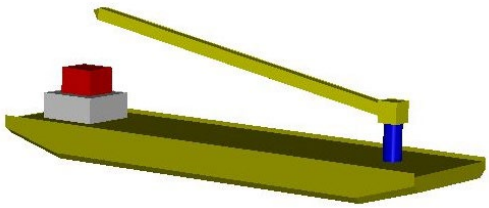

Fig. 1: Numerical model of Floating Crane Barge

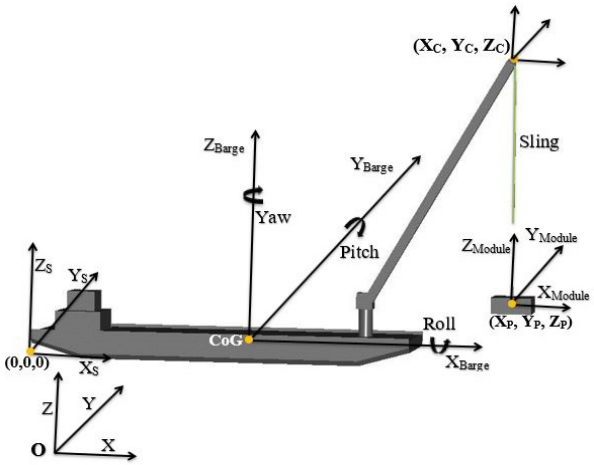

Fig. 2: Coordinate system of model

2.3 Validation

The calculation outline for coupled motion analysis on the floating crane due to the oscillation of the suspended module is described. A computer program used to construct matrix operations is easy, fast, and suitable for predicting model responses. The scheme proposed in this study is presented in Fig. 3. There are three parts to the ship motion simulation for the numerical model. Some of the required inputs to run the program are aspects of floating crane barges, mooring restoring forces, suspended modules, and coupling stiffness. Based on data from the properties of crane barges, hoisting wire, and viscous damping.

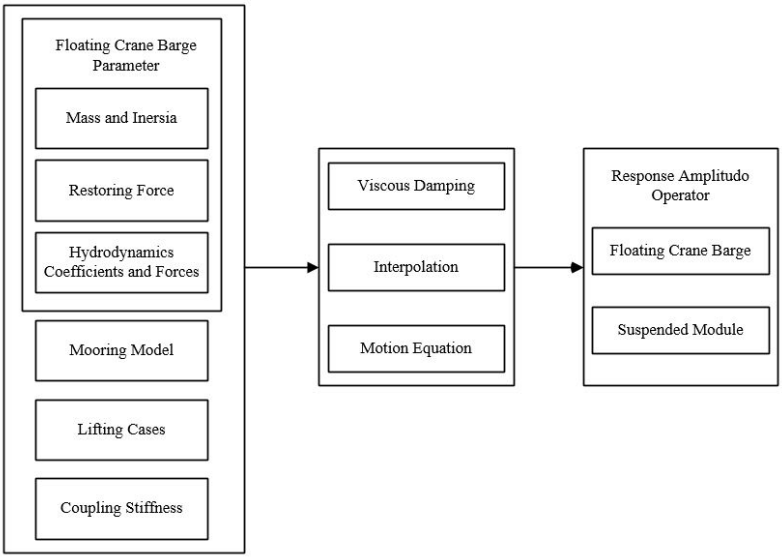

Fig. 3: Scheme of calculated simulation

Table 2. Numerical properties of Floating Crane Barge and Suspended Module

Parameter	**Symbol**	**Value**
Floating Crane Barge		
Length overall (m)	L_{OA}	84
Breadth molded (m)	B_m	21
Height (m)	H	6
Draft (m)	T	2.5
Displacement mass (kg)	Δ_{Ms}	3.469E+6
Vertical center of gravity above baseline (m)	VCG	3.836
Longitudinal center of gravity from AP (m)	LCG	43.785
Body origin in global coordinate (m)	(x_s, y_s, z_s)	(0, 0, 0)
Inertia Moment x- direction (kgm^2)	I_{XX}	2.56E+8
Inertia Moment y- direction (kgm^2)	I_{YY}	1.56E+9
Inertia Moment z- direction (kgm^2)	I_{ZZ}	1.86E+9
Crane of tip relative position to CoG (m)	(x_c, y_c, z_c)	(53.452, 0.01, 43.79)
Suspended Module		
Length (m)	L_M	4.2
Breadth (m)	B_M	4.2
Height (m)	H_M	2.0
Displacement mass 1 (kg)	Δ_{Ml1}	1.2E+5
Displacement mass 2 (kg)	Δ_{Ml2}	2.4E+5
Relative position to CG (m)	(x_p, y_p, z_p)	(53.452, 0.01, 7.08)
Rope		
Length of the outstretched (m)	l_s	34.00
Diameter (m)	D	5.14E-2

The original database for computing coupled motion can be interpolated using an interpolation technique. Then, all parameters can be entered into the coupled motion equation as in Equation 1. The linear transfer function of a floating crane barge and suspended module can be obtained from the derivation of the motion equation.

The verification of the simulation model is required as a confirmation process in the application of equations following the conceptual model related to numerical

simulation. The model input includes several relatively simple parameters and complex numerical operations. The script module of computer programs can be made simpler and easier. In this verification, the RAO calculations of the floating crane are carried out without involving the suspended module. The most important output of the simulation model is the amplitude-frequent resonance of the 6 DOF motion responses. The results of the simulation model are validated with the computational output of the ANSYS AQWA program. The hydrodynamic analysis for the floating barge is generated by the potential flow theory before the response analysis of the coupled system. The meshing model was created with a maximum element size of 1.0 m and a defeating tolerance of 0.24 m using the square meshing type. The water depth was 70 m.

In the simulation model for this verification, the motion responses of the floating crane barge were just considered by the beam sea. The coupled analysis of floating crane barge motion for the model verification is computed numerically in the ballast condition and free-floating. The comparison of the RAO model with ANSYS AQWA can be observed in Fig. 4. In general, The RAO result of the floating barge for all six DOF modes indicates a good agreement between the present model and the output of ANSYS AQWA. Therefore, the accuracy of the calculation on the numerical model shows that the results are well-validated. In addition, the analysis of the simulation model results on the responses of floating crane barges without a module load is compared directly with the experimental results based on the basin test. The predictions of simulation models for solving research problems require direct verification with data from experimental or observational tests[20–25].

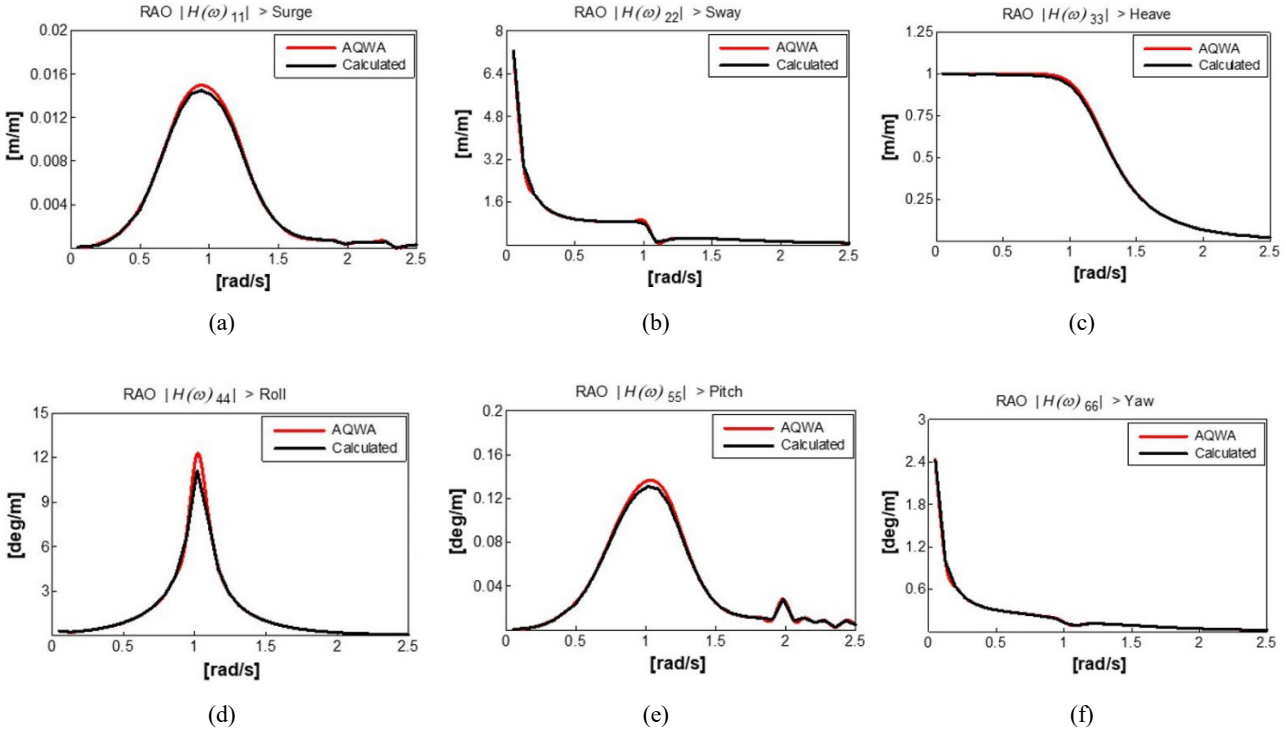

Fig. 4: Numerical calibration of RAO model for (a) surge, (b) sway, (c) heave, (d) roll, (e) pitch, (f) yaw.

The characteristics of the RAO curve in the simulation model and ANSYS AQWA can be analyzed in more detail. The peak response of the RAO curve can be seen clearly between the red and black lines. The red line indicates the response of ANSYS AQWA, while the black line shows the response of the simulation model. At the peak frequency in almost all degrees of freedom, these lines have different response values. The apparent difference is understood to because the simulation model applied an additional equation as the viscous damping value. The total damping coefficient in the simulation model is greater than the reference input, and the response on the peak frequency of RAO is slightly smaller than ANSYS AQWA. According to Zaraphonitis and Papanikolaou[26], in some cases, ship motion prediction at the resonant frequency was an overestimation. Problems arise in numerical prediction due to nonlinear effects on hydrodynamic coefficients, such as damping coefficients. The ship model's performance was highly dependent on the hydrodynamic effect[27].

3. Result and Discussion

The coupled motion analysis on the floating crane and suspended module using the empirical model proposed in this article is performed during lifting operations under standby conditions. The fixed position of the suspended module for the simulation model is only placed at the stern, center, and amidships, and the crane doesn't rotate. The hoisting crane during the lifting process is simulated,

assuming a single crane lift. In the present study, wave-induced force relative to the floating barge is only considered as a 90-degree beam wave. The simulation model presents the motion response characteristics of the multibody under different load conditions.

The simulation results for the translational motion response of a floating crane barge are presented in Fig. 5. The solid black lines indicate the calculated motion response without load, and the black square marks indicate the experimental motion response without load. The red short dash lines indicate the motion response of a suspended load of about 3.3%, and the blue short dash lines indicate the motion response of a suspended load of about 6.7%. It can be observed that the RAO curve of the surge, sway, and heave motion at load conditions is between 3.3% and 6.7%, with a small difference in response characteristics. The first peak responses on the surge and sway motion at a low frequency of about 0.22 rad/s are affected by the frequent resonance of the mooring stiffness. The obvious discrepancy in the RAO curves with and without a suspended module load occurred at a peak frequency of about 0.57 rad/s. The phenomenon of peak responses in the RAO curve with load is caused by the frequent resonance of the swinging movement in the suspended module. This phenomenon occurs as well as the RAO curve of the heave motion; the results with suspended loads indicate the largest response peak at a frequency of about 0.57 rad/s. Then, the peak response begins to decrease again, close to the RAO value of about 1 m/m at lower frequencies.

The apparent peak frequency of the floating crane response due to the swinging load can be explained by a theoretical approach to the physical mass-spring system. The swinging load on the crane lift is assumed to be a hanging system, and the natural frequency (ω_n) of suspended module movement can be estimated using the theoretical basis of a simple pendulum system. So, the natural frequency calculation of suspended modules in horizontal movement can be approximated based on the following equation:

$$\omega_n = \sqrt{\frac{g}{l_s}} \tag{15}$$

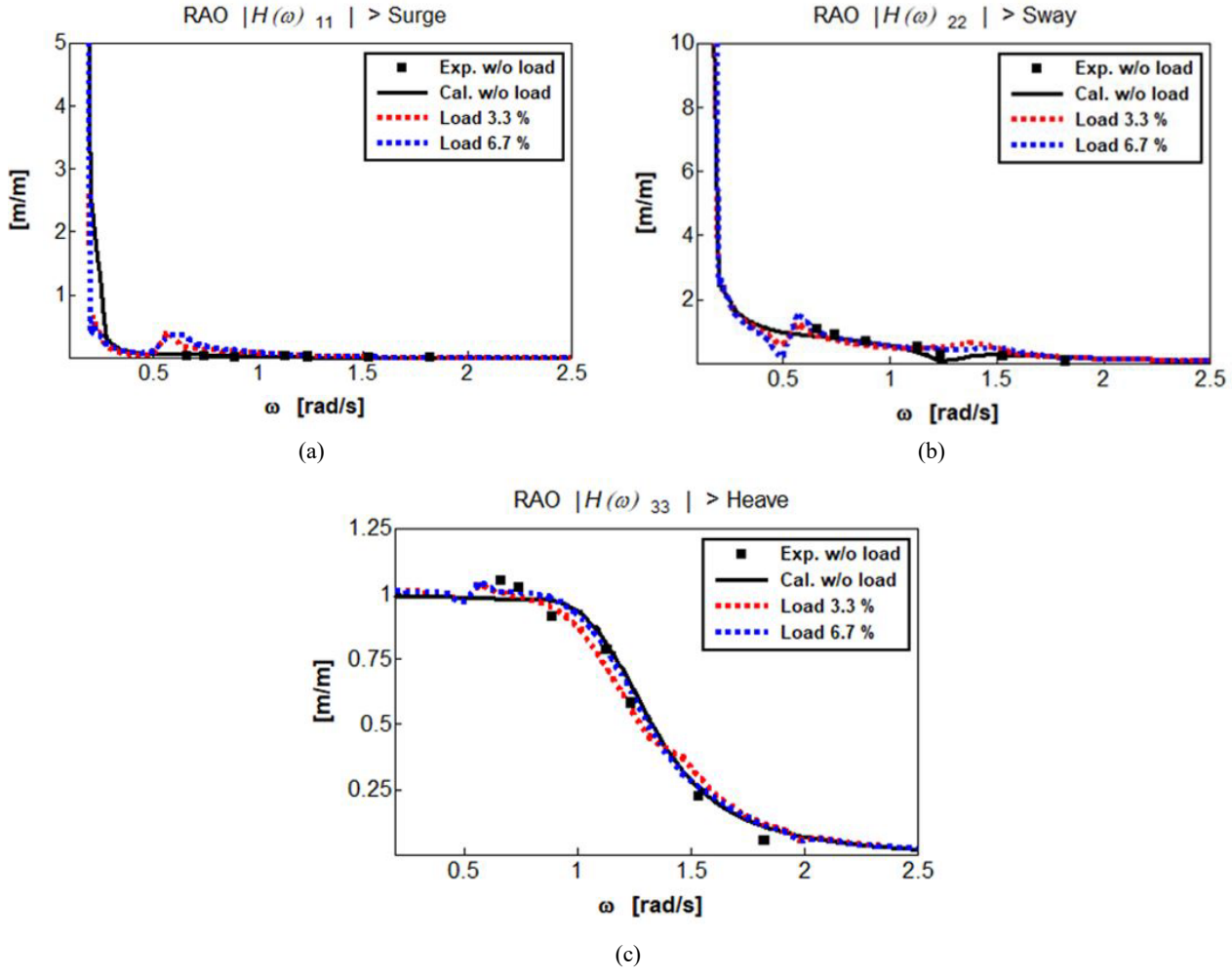

Fig. 5: RAO of Floating Crane Barge for (a) surge, (b) sway, (c) heave.

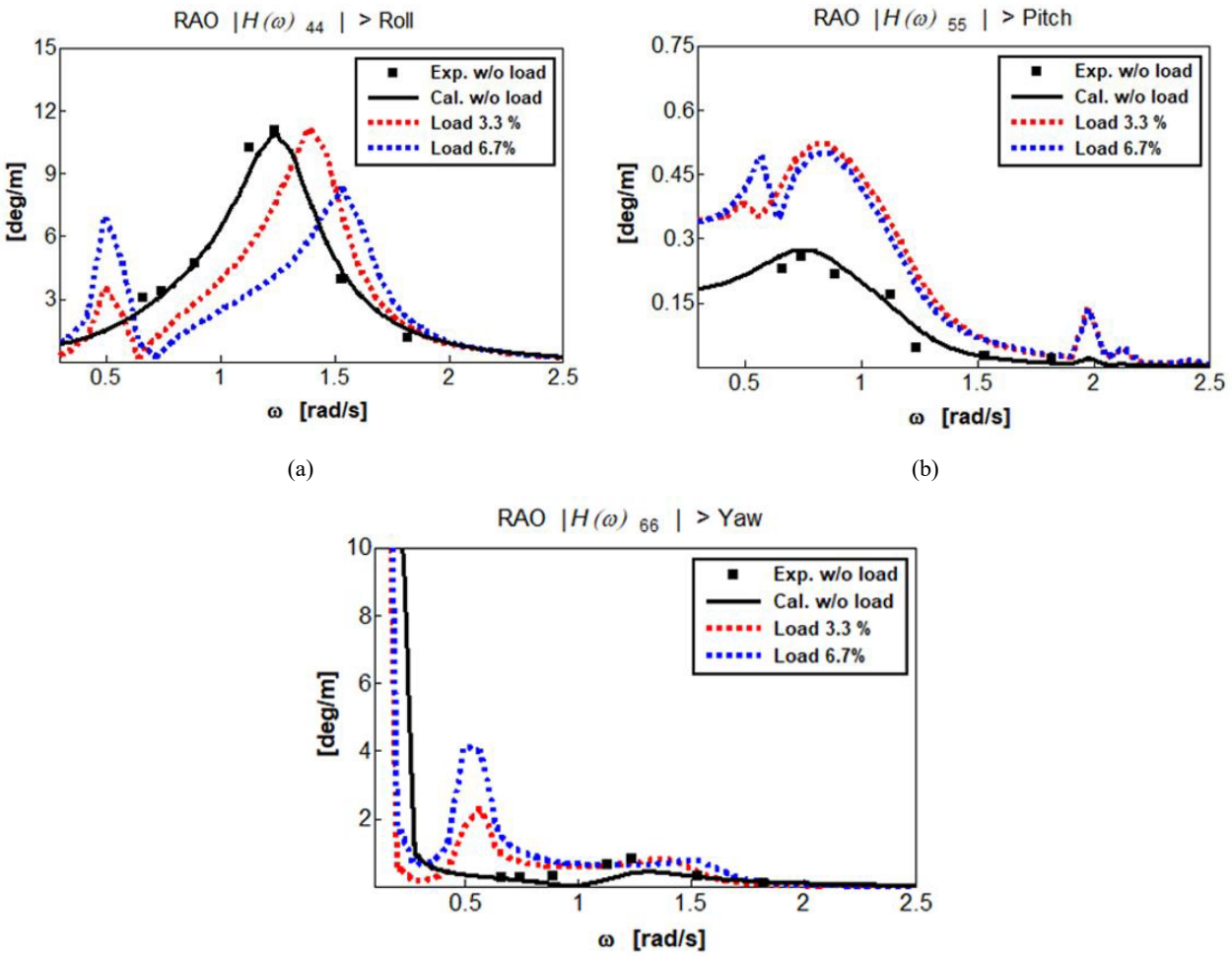

Fig. 6: The RAO of Floating Crane Barge for (a) roll, (b) pitch, (c) yaw.

Fig. 6 indicates the results of the coupled motion response on the rotational RAO curve of the floating crane barge. In general, the frequent resonance affected by the swinging movement of the pendulum at a frequency of about 0.57 rad/s occurred in the roll, pitch, and yaw peak responses of a floating crane barge with a suspended load. It can be clearly seen that the peak response caused by the pendulum resonance of the suspended load for all rotational motion increases if the weight of the suspended module gets heavier. This peak response on the load case of 6.7% for the roll and yaw motion is more than twice the response on the load case of 3.3%.

In particular, the enhancement of peak response for the pitch motion is not as significant as for the other two rotational motions. It can be understood that the wave load on the beam sea causes a small swinging movement of the suspended module in the x-direction. In this study, the horizontal movement in the x-direction is greatly influenced by the pitch motion response of a floating crane. The biggest pitch response in the load of 3.3% is founded at the third peak frequency of around 1.15 rad/s. This peak response is due to the frequent resonance from the vertical or z-direction of the module movement. The case study in this simulation model assumes that the mass of the hanging point has a big impact on the floating crane's response during the lifting operation in waves. Moreover, the coupling interaction between the floating crane and module is triggered by the swinging movement of the crane boom, connecting the crane tip with the hanging system.

The peak response roll motion shifts at a higher frequency if the floating crane is given a suspended load. The comparison of dynamic response spectra between floating cranes with and without a suspended load based on a model test showed that there was a shifting of natural frequency on the roll motion. While the natural frequency of pitch motion, both with and without a suspended load, tends to shift very little and occur at a frequency of around 0.9 rad/s, The frequent resonance of roll motion with a larger suspended module is a higher frequency than a small module. The peak frequency without a suspension due to the resonance of frequency occurs at a frequency of about 1.2 rad/s. While peak frequencies for loads of 3.3% and 6.7% occur at frequencies of about 1.34 rad/s and 1.51 rad/s, It can be observed that the increasing natural frequency is caused by the decreasing inertia moment of roll due to the external moment influenced by the hoisting system. The decreasing inertia moment of the rolling

generates a fast oscillating period on the system's motion with a pendulum. It can be explained that a change in displacement of the vessel can affect a shifting of the gyration radius on the roll motion. The peak response of a larger suspended load on the roll motion is getting smaller than that of a small suspended load. In addition to being affected by the damping coefficient, the dynamic responses of floating cranes on the multibody system are significantly induced by the dynamic response of a swinging pendulum. According to the experimental study[8,12], the oscillation of swinging suspended objects influenced the obstructed roll motion in beam seas.

For the lifting and lowering processes in offshore activities, one part of the system being analyzed is the behavior of the suspended load response in the hanging system. The characteristics of a lifted object are generally investigated in terms of the acceleration level parameter. The assessment of the response acceleration during operation will relate to the practical calculation of the mass force and the dynamic amplification factor (DAF) in the crane boom. In this article, the dynamic responses of the suspended module were presented in the acceleration RAO shown in Fig. 7.

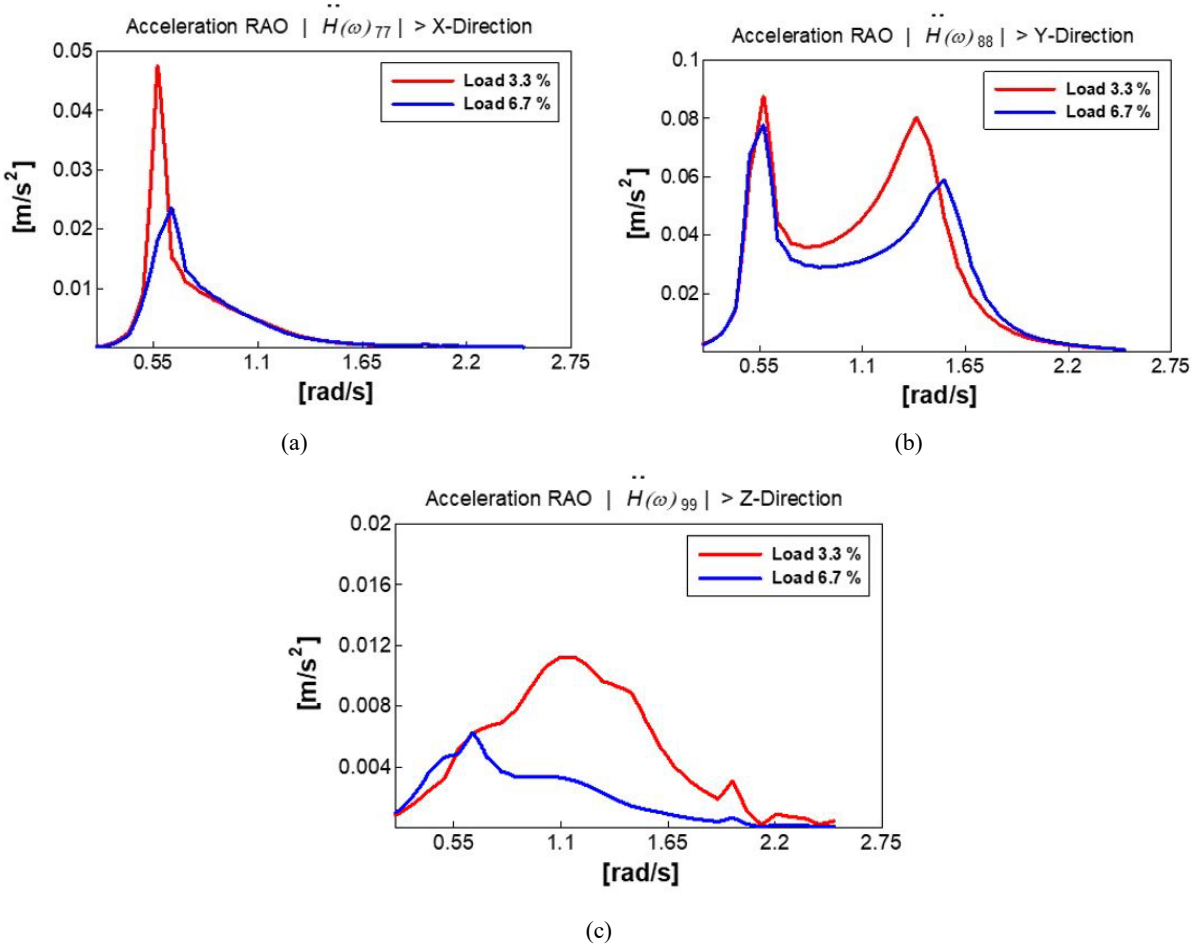

Fig. 7: Acceleration RAO of Suspended Module movement for (a) x-direction, (b) y-direction, (c) z-direction.

The peak frequency of module acceleration in x, y, and z directions at a frequency of about 0.57 rad/s is strongly influenced by the resonance near the natural frequency of horizontal movement. For the RAO curve in the x-direction, the peak response on the large module has decreased by more than two times compared to the small module. This result is caused by the restoring force of the hoisting rope on the small module, which is smaller than the large module. In this simulation, the structural damping on the hoisting system is assumed to be almost the same. Based on the derivation of the linear motion equation using the frequency domain, it states that the response value is inversely proportional to the mass and the restoring force. This behavior also applies to both suspended module responses in the y- and z-directions. This can be seen clearly in the acceleration RAO curve in Fig. 6.

The peak response of the swinging module for the y-direction is getting higher than the x- and z-directions. Based on the theory of vessel motion response relative to the beam sea heading, the biggest response occurred in roll motion[28]. In the floating crane, the horizontal module movement in the y-direction is influenced predominantly by the ship's roll motion through the swinging of the crane boom. This response characteristic was described by the appearance of the resonant phenomenon that the second

peak responses of the acceleration RAO curve in the y-direction were induced by the frequent resonance of the vessel roll motion. For the module response in the z-direction, the RAO curve of the small module indicates a great response caused by the resonance of vertical movement at a frequency of about 1.15 rad/s. It is understood that the module with a smaller mass tends to oscillate more easily than a heavier mass in the coupling motion of the hanging system. In contrast, a heavier suspended module tends to create a rigid body system in combination with the crane tip and the hanging rope.

4. Conclusion

The development of a simulation model in the frequency domain is performed by empirical calculations that aim to predict the coupled motion responses between the floating crane and the suspended module during lifting operations. From the results of the simulation model that has been described in this article, some conclusions can be drawn as follows:

1. The peak frequency generated by the frequent resonance of the suspended module swinging appears clearly in all the motion responses of the floating crane barge. The peak responses caused by the resonance of module movement in the rotational motions tend to increase with increasing the weight of the suspended module. Meanwhile, the peak response of the suspended module caused by the resonance of floating crane barge motions only occurs in the horizontal movement in the y-direction for the beam sea.
2. The natural frequency of roll motion on the floating crane barge with a suspended module is higher than without a suspended module. The peak frequency of roll motion during the lifting process shifts to a higher frequency as the weight of the suspended module increases.
3. The response of suspended module acceleration in all directions for a larger mass is lower than for a smaller mass.

In order to determine the effect of nonlinear response on multibody systems, it is necessary to develop further simulation models for the prediction of couple motion during lifting operations using the time domain method. In addition, further research is needed regarding the tension response of the mooring and the crane rope during the module lifting process.

Acknowledgments

The author would like to thank the National Research and Innovation Agency (BRIN) for providing facilities to support this research. The authors also thank the Deputy for Infrastructure Research and Innovation – (BRIN) for supporting ANSYS AQWA Simulation. This work is part of the FOWT research activity "Development of Floating Offshore Wind Turbine for Power Generation Based on Model Test" research grand DIPA-124.01.1.690505/2023 conducted by the Marine Renewable Energy Conversion Technology research group, Research Center for Hydrodynamics Technology, National Research and Innovation Agency (BRIN).

Nomenclature

A	hydrodynamic added masses (N/(m/s^2) or N m /(deg/s^2))
A_0	area of wire rope (m^2)
B	hydrodynamic damping (N m /(deg/s^2) or N m /(deg/s))
B_m	breadth moulded of barge (m)
B_v	viscous damping (N m /(deg/s))
C_c	linearized coupling stiffness (N/m)
c_{c44}	force due to coupling stiffness in roll/roll (N m)
c_{c55}	force due to coupling stiffness in pitch/pitch (N m)
c_{c66}	force due to coupling stiffness in yaw/yaw (N m)
C_f	filling coefficient rope
C_h	hydrostatic stiffness (N/m)
C_m	linearized mooring stiffness (N/m)
CoG	center of gravity
D	diameter of hoisting rope (m)
DAF	dynamic amplification factor
DOF	degree of freedom
E	young's modulus (Pa)
F_w	exciting force (N)
g	acceleration of gravity (m/s^2)
H	height of barge (m)
I_{xx}	inertia moment x-direction (kgm^2)
I_{yy}	inertia moment y-direction (kgm^2)
I_{zz}	inertia moment z-direction (kgm^2)
k_e	vertical stiffness due to axial rope (Pa/m)
k_s	horizontal stiffness due to gravity (N/m)
LCG	longitudinal center of gravity (m)
l_e	effective elastic length of rope (m)
l_s	length of the outstretched rope (m)
L_{OA}	length overall of barge (m)
M	total masses and inertia (N/(m/s^2) or N m /(deg/s^2))
M_L	mass of suspended module (N/(m/s^2))
M_S	inertia moment y-direction (kgm^2)
O	earth-fixed frame
RAO	response amplitude operator
T	draft (m)
ν	damping ratio (%)
VCG	vertical center of gravity (m)

ω	wave frequency (rad/s)
ω_n	natural frequency (rad/s)
x_c	coordinate point of crane tip relative CoG in x-direction (m)
x_p	coordinate point of module relative CoG in x-direction (m)
y_c	coordinate point of crane tip relative CoG in y-direction (m)
y_p	coordinate point of module relative CoG in y-direction (m)
z_c	coordinate point of crane tip relative CoG in z-direction (m)
z_p	coordinate point of module relative CoG in z-direction (m)

References

1) M.H. Huzaifi, M.A. Budiyanto, and S.J. Sirait, "Study on the carbon emission evaluation in a container port based on energy consumption data," *Evergreen*, **7**(*1*) 97–103 (2020). doi:10.5109/2740964.
2) L. Sun, R. Eatock Taylor, and Y.S. Choo, "Multibody dynamic analysis of float-over installations," *Ocean Eng.*, **51** (*May*) 1–15 (2012). doi:10.1016/j.oceaneng.2012.05.017.
3) Jaswar, K.U. Tiau, H. Abyn, and C.L. Siow, "Stability of mobile floating harbor container crane," *J. Teknol.* , **66** (*2*) 2180–3722 (2014). www.jurnalteknologi.utm.my.
4) N. Firdaus, E. Budi Djatmiko, R. Walujo Prastianto, and D. Muhammad Fajariansyah Ismail, "ANALISIS respon gerak floating crane barge untuk decommissioning struktur lepas pantai motion response analysis of a floating crane barge for the decommissioning of offshore structures," *J. Ilm. Teknol. Marit.*, **15** (*1*) 31–44 (2021).
5) P.K. Mukerji, "Hydrodynamic Responses of Derrick Vessels in Waves During Heavy Lift Operation," in: Offshore Technol. Conf., 1988: pp. 149–154.
6) J. Baar, J. Pijfers, S. Intl, P.B. Mij, and A. van Santen, "Hydromechanically Coupled Motions of a Crane Vessel and a Transport Barge," in: Offshore Technol. Cenference, 1992: pp. 31–49.
7) L. Li, Z. Gao, T. Moan, and H. Ormberg, "Analysis of lifting operation of a monopile for an offshore wind turbine considering vessel shielding effects," *Mar. Struct.*, **39** 287–314 (2014). doi:10.1016/j.marstruc.2014.07.009.
8) N. Firdaus, E.B. Djatmiko, R.W. Prastianto, and Muryadin, "Experimental Study on Coupled Motion of Floating Crane Barge and Lifted Module in Irregular Waves," in: IOP Conf. Ser. Earth Environ. Sci., 2022. doi:10.1088/1755-1315/972/1/012070.
9) J.A. Witz, "PARAMETRIC excitation of crane loads in moderate sea states," *Ocean Eng.*, **22** (*4*) 411–420 (1995).
10) M.M. Idres, K.S. Youssef, D.T. Mook, and A.H. Nayfeh, "A NONLINEAR 8-DOF COUPLED CRANE-SHIP DYNAMIC MODEL," in: 44th AIAA/ASME/ASCE/AHS Struct. Struct. Dyn. Mater. Conf., Aerospace Research Central, Norfolk, Virgina, 2003: pp. 1–11.
11) V. Čorić, I. Ćatipović, and V. Slapničar, "FLOATING crane response in sea waves," *Brodogradnja/Shipbuilding*, **Vol. 65 No.2** 111–122 (2014).
12) Y. Chen, L. Ma, W. Duan, and P. Liu, "Experimental study on coupled motions of mother ship launching and recovering of human-occupied vehicle in regular waves," *J. Mar. Sci. Appl.*, **19** (*1*) 53–63 (2020). doi:10.1007/s11804-019-00114-5.
13) S. Oh, T. Utsunomiya, and K. Saiki, "On-site measurement and numerical modelling of a lifting operation for caissons using floating crane," in: Proc. Int. Conf. Offshore Mech. Arct. Eng. - OMAE, OMAE2018-77132, Madrid, 2018: pp. 1–6. doi:10.1115/OMAE2018-77132.
14) C.L. Siow, J. Koto, H. Abby, and N.M. Khairuddin, "Prediction of semi-submersible's motion response by using diffraction potential theory and heave viscous damping correction," *J. Teknol.*, **69** (*7*) 2180–3722 (2014). www.jurnalteknologi.utm.my.
15) L. Bergdahl, "W ave-Induced Loads and Ship Motions," Goteborg, 2009.
16) A. ANSYS, "AQWA Theory Manual," Canonsburg, PA, 2015. http://www.ansys.com.
17) D. Norske Veritas, "RECOMMENDED PRACTICE DET NORSKE VERITAS AS Modelling and Analysis of Marine Operations," 2011. http://www.dnv.com.
18) F. Aliunir, T.Y.M. Zagloel, and R. Ardi, "Discrete-event simulation and optimization of spare parts inventory and preventive maintenance integration model considering cooling down and machine dismantling time factor," *Evergreen*, **7**(*1*) 79–85 (2020). doi:10.5109/2740949.
19) N. Kumari, K. Singh, and S. Kumar, "MATLAB-based simulation analysis of the partial shading at different locations on series-parallel pv array configuration," *Evergr. Jt. J. Nov. Carbon Resour. Sci. Green Asia Strateg.*, **9**(*4*) 1126–1139 (2022). doi:10.5109/6625724
20) S. Hironaka, Y. Fujisawa, S. Manabe, G. Inoue, Y. Matsukuma, and M. Minemoto, "Estimation of the multi-phase flow on the vertical pipe for the methane hydrate recovery," *J. Nov. Carbon Resour. Sci.*, **3** 11–16 (2011).
21) T.N. Dief, and S. Yoshida, "System identification for quad-rotor parameters using neural network," *Evergreen*, **3**(*1*) 6–11 (2016). doi:10.5109/1657380.
22) A.T. Raheem, A.R.A. Aziz, S.A. Zulkifli, A.T.

Rahem, and W.B. Ayandotun, "Development, validation, and performance evaluation of an air-driven free-piston linear expander numerical model," *Evergreen*, **9**(*1*) 72–85 (2022). doi:10.5109/4774218.
23) R. Luo, H. Zhu, and C. Hu, "A numerical investigation of an offshore overhead power transmission system," *Evergreen*, **9**(*3*) 636–644 (2022). doi:10.5109/4842521.
24) N. I. Ismail, M. Asyraf Tasin, H. Sharudin, M. Hisyam Basri, S. Che Mat, H. Yusoff, and R.E.M. Nasir, "Computational aerodynamic investigations on wash out twist morphing mav wings," *Evergreen*, **9**(*4*) 1090–1102 (2022). doi:10.5109/6625721.
25) V. Singh, V. Singh Yadav, M. Kumar, and N. Kumar, "Optimization and validation of solar pump performance by matlab simulink and rsm," *Evergr. Jt. J. Nov. Carbon Resour. Sci. Green Asia Strateg.*, **9**(*4*) 1110–1125 (2022). doi:10.5109/6625723
26) G. Zaraphonitis, and A. Papanikolaou, "On the numerical prediction of seakeeping and of structural loads of high-speed vessels," *Appl. Ocean Res.*, **26** (*6*) 274–287 (2004). doi:10.1016/j.apor.2005.08.005.
27) M.F. Syahrudin, M.A. Budiyanto, and M.A. Murdianto, "Analysis of the use of stern foil on the high speed patrol boat on full draft condition," *Evergreen*, **7**(*2*) 262–267 (2020). doi:10.5109/4055230.
28) R. Bhattacharya, "Dynamics of marine vehicles," A Wiley-Interscience publication, New York, 1978.